

RSC Advances



This is an *Accepted Manuscript*, which has been through the Royal Society of Chemistry peer review process and has been accepted for publication.

Accepted Manuscripts are published online shortly after acceptance, before technical editing, formatting and proof reading. Using this free service, authors can make their results available to the community, in citable form, before we publish the edited article. This *Accepted Manuscript* will be replaced by the edited, formatted and paginated article as soon as this is available.

You can find more information about *Accepted Manuscripts* in the [Information for Authors](#).

Please note that technical editing may introduce minor changes to the text and/or graphics, which may alter content. The journal's standard [Terms & Conditions](#) and the [Ethical guidelines](#) still apply. In no event shall the Royal Society of Chemistry be held responsible for any errors or omissions in this *Accepted Manuscript* or any consequences arising from the use of any information it contains.

Facile synthesis of enzyme-inorganic hybrid nanoflowers and their application as an immobilized trypsin reactor for highly efficient protein digestion[†]

Zian Lin,* Yun Xiao, Ling Wang, Yuqing Yin, Jiangnan Zheng, Huanghao Yang,* and Guonan Chen

Received (in XXX, XXX) Xth XXXXXXXXX 200X, Accepted Xth XXXXXXXXX 200X

First published on the web Xth XXXXXXXXX 200X

DOI: 10.1039/b000000x

A novel kind of immobilized trypsin reactor based on enzyme-inorganic hybrid nanoflowers was first developed and can be applied to ultra fast, highly efficient proteome digestion.

Nanobiocatalysis, in which enzymes are incorporated into nanostructured materials, has attracted increasing attention due to its potential applications related to catalysis, proteomic analysis, and biosensors.¹ Nanostructures, including nanoporous silica, nanofibers, nanotubes and nanoparticles, have manifested great efficiency in the manipulation of the nanoscale environment of the enzyme and thus promise exciting advances in many areas for enzyme technology.

Flower-like nanomaterials (nanoflowers), possessing of large surface-to-volume ratio compared with that of bulk materials, are not currently reported so frequently, as, for example, nanoparticles or beads due to their extremely harsh synthetic conditions. To date, although various approaches have been developed to synthesize nanoflowers, most attempts are focused on oxidation of elemental metals, reduction of metal salts, thermal decomposition of relatively unstable compounds, and electrochemical routes.² Among them, special precautions should be taken to avoid uncontrolled growth or morphological deformations since they tend to be employed with harsh conditions (high temperature and pressure and the use of toxic organic solvents). Therefore, a low cost and facile synthetic method for the preparation of controlled and well-defined hierarchical nanoflowers is still in great demand. Recently, an encouraging breakthrough in preparation of immobilized enzymes with greatly enhanced activities was achieved by Ge et al,³ who reported the synthesis of hybrid nanostructures comprising of $\text{Cu}_3(\text{PO}_4)_2$ and enzymes via a coprecipitation method. Using the same principle, Wang et al^c prepared CaHPO_4 - α -amylase hybrid nanoflowers and further interpret the mechanism for catalytic activity of immobilized enzyme. Nevertheless, so far the advantages of enzyme-inorganic hybrid nanoflowers have not been fully demonstrated. Further development is necessary to explore new benefits of this type of hybrid nanoflowers.

Mass spectrometry (MS) has been widely used to analyze biological samples and has evolved into an indispensable tool for proteomic research. Generally, MS-based approach for protein identification is carried out by analysis of enzymatically digested peptide products from the parent protein, among which more

effective proteolysis served as key step to efficiently identify proteins. The routine proteolysis of proteins is performed in solution, but it suffers from several drawbacks such as long digestion time (up to 24 h), enzyme autolysis, low stability of the enzyme to environmental changes (heat, organic solvents, or pH), and difficult recovery of enzymes.⁴ These problems can be overcome to some extent by enzyme immobilization on solid supports (referred as immobilized enzyme reactors, IMERs), which provide advantages including high enzyme-to-substrate ratio, great enzyme stability and reusability, good digestion efficiency, as well as short digestion time.⁵ Presently, numerous solid supports including commercially available beads,⁶ nanoparticles,⁷ membranes,⁸ glass,⁹ polymer- and silica-based monolithic materials¹⁰ were covalently bonded, trapped or physically adsorbed with protease have been developed as IMERs. Although these IMERs have achieved some success, additional approaches for obtaining high-efficiency IMERs are highly desirable. To our best knowledge, the advantages of the enzyme-inorganic hybrid nanoflowers as a kind of IMERs for protein digestion have not been demonstrated so far.

Herein, we report an approach for the preparation of enzyme-inorganic hybrid nanoflowers using copper (II) ions as the inorganic component and trypsin as the organic component. The synthetic method is simple and requires no harsh conditions. The as-prepared hybrid nanoflowers have an interesting structure containing of micrometre-sized particles and nanoscale flower-like petals. Significantly, the hybrid nanoflowers, applied as a novel IMER, exhibit higher proteolytic performance than the free enzyme. As illustrated in Fig.1(a), the hybrid nanoflowers were synthesized in one pot by adding 20 μL of aqueous CuSO_4 (120 mM) solution to 3 mL of PBS solution containing trypsin, at pH 7.4. After room-temperature incubation for 3 day, a blue precipitate with porous, flower-like structures appeared. Fig.1 (b-d) showed the SEM images of the trypsin-inorganic nanoflowers. In the low-resolution SEM images, most of the hybrid nanoflowers were uniform (Fig.1(b-c)). The high-resolution SEM image (Fig.1(d)) showed that the hybrid nanoflowers have a hierarchical peony-like flower morphology, which was assembled from hundreds of nanoplates (the lower right of Fig.1 (d)). For example, the average diameter of a single nanoflower was $\sim 40 \mu\text{m}$ was obtained while using 0.5 mg mL^{-1} trypsin.

The effect of trypsin concentration on the formation of hybrid nanoflowers was investigated (Fig.2). In the absence of trypsin, large crystals, but no nanoflowers, are formed (Fig.2(A)). However, the flower-like nanostructures emerged when trypsin was added. The nanoflowers (Fig.2(B)) with a diameter $\sim 40 \mu\text{m}$ formed many slices that resembled the petals of flowers with rough fringes when the concentration of trypsin was in the range of $0.02\sim 0.5 \text{ mg mL}^{-1}$. Gradually increasing the concentration of trypsin ($0.5\sim 5.0 \text{ mg mL}^{-1}$), the morphologies of the nanoflowers changed significantly, and

Ministry of Education Key Laboratory of Analysis and Detection for Food Safety, Fujian Provincial Key Laboratory of Analysis and Detection Technology for Food Safety, Department of Chemistry, Fuzhou University, Fuzhou 350116 (China), Fax: +86-591-22866135 E-mail: zianlin@fzu.edu.cn (Z.A. Lin); hhyang@fzu.edu.cn (H.H. Yang)

[†] Electronic Supplementary Information (ESI) available: Experimental details and additional figures. See DOI: 10.1039/c0xx00000x

reversely mimicking the growth process of flowers in nature was observed from small bud to bloom (Fig.2(C-D)). Correspondingly, the average diameters of these nanoflowers decreased from $\sim 40 \mu\text{m}$ to $\sim 5 \mu\text{m}$. The results demonstrated that the formation and size of the nanoflowers were strongly dependent on trypsin concentration added in the synthesis. It should be noted that the morphological structure of the nanoflowers was also determined by the molecular weights of proteins. For example, the hierarchical shrubalthea-like and rose-like nanoflowers were obtained (Fig.S1, ESI[†]) using 2.0 mg mL^{-1} Lyz and 0.1 mg mL^{-1} IgG as model proteins, respectively.

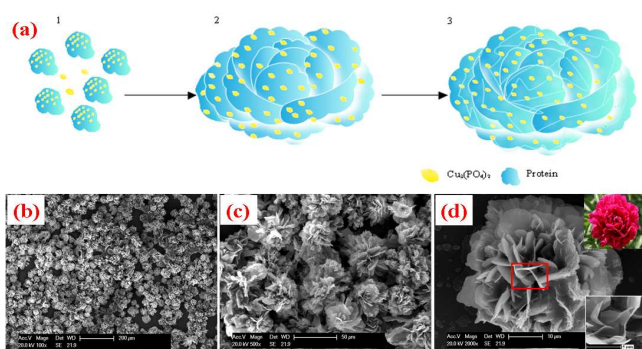


Fig.1 (a) Schematic representation of the synthesis of hybrid nanoflowers; (b-d) SEM images of the hybrid nanoflowers obtained from an aqueous solution of 0.5 mg mL^{-1} trypsin, 120 mM Cu^{2+} , 0.1 M PBS at pH 7.4.

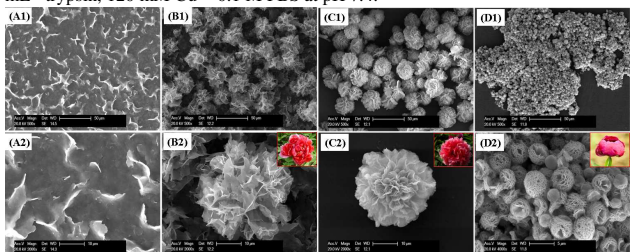


Fig.2 Effect of different trypsin concentrations on the morphologies of nanoflowers. (A1-2) 0.0 mg mL^{-1} ; (B1-2) 0.02 mg mL^{-1} ; (C1-2) 1.0 mg mL^{-1} ; (D1-2) 5.0 mg mL^{-1} .

To gain deeper insight into the growth mechanism of the hybrid nanoflowers, SEM images were recorded as a function of nanoflower growth time. For this series of experiments, we carried out the experiment in identical concentrations (120 mM Cu^{2+} , 0.1 M PBS at pH 7.4, 0.5 mg mL^{-1} trypsin, and reaction at room temperature), but for different incubation time. As presented in Fig.S2 (ESI[†]), at an early growth stage (24 h , Fig.S2(A)), primary crystals of $\text{Cu}_3(\text{PO}_4)_2$ were formed. At this stage, trypsin formed complexes with Cu^{2+} predominantly through coordination of the amide groups in the enzyme backbone. These complexes provided a location for nucleation of the primary crystals. With increasing incubation time (48 h , Fig.S2(B)), trypsin- Cu^{2+} crystals combined into large agglomerates that formed the primary petals. The kinetically controlled growth of $\text{Cu}_3(\text{PO}_4)_2$ crystals originated on the surface of these agglomerates, resulting in flower-like petals to appear in embryo. Anisotropic growth led to complete formation of a branched flower-like structure when the incubation time reached 72 h (Fig.S2(C)). In this growth process, trypsin induced the nucleation of the $\text{Cu}_3(\text{PO}_4)_2$ crystals to form the scaffold for the petals, and also served as a "glue" to bind the petals together. Besides, we also investigated the effect of incubation temperature on the morphology of the nanoflowers. By comparison with room-temperature reaction ($25 \text{ }^\circ\text{C}$), the incubation at $0 \text{ }^\circ\text{C}$ did not result in highly branched nanoflowers with high yield (Fig.S3, ESI[†]). Obviously, lower growth rate can respond to the above results, and thus causes the uncompleted formation of a branched flower-like structure.

FT-IR spectroscopy provides a direct proof for the synthetic process of the hybrid nanoflowers (Fig.S4, ESI[†]). Compared to spectrum a and b, the typical bands of trypsin at $1400\text{--}1600 \text{ cm}^{-1}$ for $-\text{NH}_2$, and $2800\text{--}3000 \text{ cm}^{-1}$ for $-\text{CH}_2$ and $-\text{CH}_3$ were observed in spectrum c. Moreover, the hybrid nanoflowers in spectrum c did not show new adsorption peaks and significant peak shift, indicating trypsin was immobilized via self-assembly, instead of covalent bonding. X-ray diffraction (XRD) analysis (Fig.S5, ESI[†]) confirmed the nanoflowers were well crystallized and had high crystallinity after incorporating trypsin. In addition, the surface area, pore volume and average pore diameter were measured using the BET method and the corresponding values were $31.5 \text{ m}^2 \text{ g}^{-1}$, $0.094 \text{ cm}^3 \text{ g}^{-1}$ and 12.1 nm , indicating the presence of the porous structure and high surface-to-volume ratio in the hybrid nanoflowers. The actual encapsulation efficiency (defined as the ratio of the amount of immobilized trypsin to the total amount of trypsin employed) and weight percentages of trypsin in the nanoflowers were further determined by colorimetric and gravimetric methods, respectively. The results (Table S1 and S2, ESI[†]) demonstrated the encapsulation yield was over 79% when the concentration of trypsin was less than 0.1 mg mL^{-1} . In this instance, weight percentage of trypsin in nanoflowers was not more than 9.0%. However, excessive addition of trypsin to a constant inorganic component may induce the dramatic decrease of encapsulation efficiency, where only 12.5% of encapsulation yield was obtained as the trypsin concentration was 0.5 mg mL^{-1} , but a relatively higher weight percentage of 12.6% was achieved in comparison to those obtained in the low concentrations of trypsin. The results were in accordance with the previous report.³ Based on the above results, the hybrid nanoflowers with 0.5 mg mL^{-1} trypsin was chosen as the best for further evaluation and applications considering its good morphology and high weight percentage.

The catalytic activity of the hybrid nanoflowers was evaluated using N_α -benzoyl-L-arginine ethyl ester (BAEE) as the substrate according to the method described previously.¹¹ It is known that trypsin catalyzes the hydrolytic cleavage of the ester linkage in BAEE to generate N_α -benzoyl-L-arginine (BA), together with appearance of an absorbance peak at 253 nm . This phenomenon allows us to monitor the kinetics of the reaction by colorimetric method. The absorbance of different systems (nanoflowers and free trypsin) at BA peak along time is demonstrated in Fig.3(A). The plot lies on the premise of setting equivalent initial concentrations of BAEE to 0.5 mM . Upon the addition of free trypsin, absorbance at 253 nm increased slowly and reached the platform over 10 min . However, in trypsin-embedded nanoflower system (the concentrations of trypsin put in were all 1.25 mg mL^{-1}), same absorbance of BA could be obtained within 2 min , indicating the high catalytic efficiency of the nanoflowers. The pseudofirst-order kinetics with respect to BAEE could be applied to our experimental system. As shown in the insert part of Fig.3(A), the approximately linear shape of the plot of $-\ln I_{\text{sub}}$ (I_{sub} is the value obtained by subtracting the real-time absorbance from the saturated one) vs time supports the pseudofirst-order assumption. Based on it, the average reaction rate constants (k) were calculated to 1.69 min^{-1} and 0.378 min^{-1} when nanoflowers and free trypsin were used, respectively. In addition, the enzymatic activity of the trypsin-embedded nanoflowers was determined to be 4689 U mg^{-1} , approximately 270% higher than free trypsin in solution (1713 U mg^{-1}). Although the increased extent of enzymatic activity is low compared to the previous work,³ where 650% enhancement in enzymatic activity was obtained using laccase-embedded hybrid nanoflowers, it is guessed that the increased extent was dependent not only on the morphology of nanoflowers, but also on the quality of enzyme used. It should be noted that the collapse nanoflowers by the addition of EDTA to remove the Cu^{2+} could not result in any

enhanced enzymatic activity. Overall, the enhancement in the enzymatic activity of trypsin-embedded nanoflowers compared to free trypsin catalysis can be ascribed to (1) minimization or elimination of autolysis of trypsin and (2) the possible stabilization of nanoflower-like structure of trypsin with high surface area and confinement, resulting in higher accessibility of the substrate to the active sites of the enzyme.

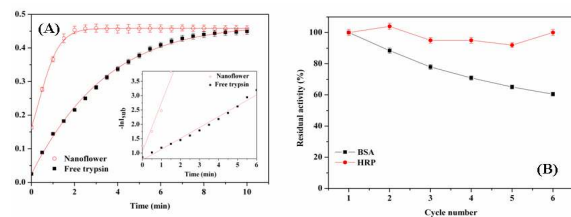


Fig.3(A) Catalytic kinetics and reaction rate (insert part) of the esterlysis of BAAE by free trypsin and hybrid nanoflowers. (○) hybrid nanoflowers; (■) free trypsin. **(B)**

Effect of recycling on the activity of hybrid nanoflowers. (●) HRP; (■) BSA

The performance of the nanoflower-based reactor was evaluated by digesting 150 pmol BSA and 200 pmol HRP, respectively. Table 1 listed the database searching results of BSA and HRP digested in solution and by the trypsin-embedded nanoflower reactors. It was observed from Table 1 and Table S3 (ESI[†]) that the total sequence coverage and the number of matched peptides for BSA obtained with the nanoflower reactor was found to be 86% and 70, comparable with those obtained in solution, where the sequence coverage of 92 % and 72 matched peptides were detected, indicating that good cleavage specificity of trypsin was remained after immobilization. However, reaction time was dramatically shortened to 1/720 (1 min vs 12 h), demonstrating that the nanoflowers have superior characteristics toward protein digestion. Compared with other immobilized trypsin reactors^{8b,12} and commercially available beads,¹⁰ the nanoflower-based IMER could offer high enzymatic activity and ultra fast digestion speed, which confirmed the superiority of the nanoflower-based reactor. It was also noteworthy that high level of sequence coverage and matched peptides can be achieved even though the nanoflowers were stored at -20 °C for 20 days, which showed the excellent stability of such nanoflower reactors. Similar results (Table 1 and S4, ESI[†]) were obtained using HRP as target protein, where 19 matched peptides with the sequence coverage of 41% could be obtained within 1 min, higher than that performed in solution digestion (14 matched peptides with the sequence coverage of 45%).

Table1. Comparison of the efficiency of hybrid nanoflower reactors and solution digestion method on protein proteolysis (n=3)

Methods	BSA digestion			HRP digestion		
	Sequence coverage [%]	Peptide matches	MS signal intensity [%]	Sequence coverage [%]	Peptide matches	MS signal intensity [%]
Free trypsin ^a	92	72	100	45	14	100
Nanoflowers ^b	86	70	93.5	41	19	91.1
Nanoflowers ^c	80	68	86.9	41	16	91.1

a) 12 h of digestion at 37 °C; b) 1 min of shake-assisted digestion on at 37 °C; c) nanoflowers were stored at -20 °C for 20 days

The feasibility of the nanoflower-based reactor for complex biological sample was demonstrated by digesting human serum. Totally, 27 proteins (most of high-abundance proteins, e.g. HSA, IgG) were identified within 1 min digestion by the reactor (n=2), even 26 proteins were found when the nanoflowers were used that was stored at -20 °C for 20 days, better than that obtained by in-solution digestion (12h), where only 21 proteins were discovered (n=2). It was clearly observed (Table S5-7, ESI[†]) that some new proteins were detected by using the nanoflowers except for the overlaps, indicating the good practicability of the nanoflowers for the digestion of complex sample.

The reusability and stability of the nanoflowers were tested by batch hydrolysis of BSA and HRP solution. To avoid the loss of nanoflowers during washing process, a home-made digestion device was recommended as depicted in Fig.S6 (ESI[†]). It was observed from Fig.3(B) that the residual activity of the nanoflower toward BSA decreased slightly as the cycle number increased, although they still showed a higher degree of activity recovery after six cycles. But a relatively high-level activity of the nanoflowers toward HRP was maintained in the studied cycles. The results suggested that the decrease of BSA in activity must not come from the loss of immobilized trypsin during the eluting process, eventual trypsin leakage, conformation changes and so on. The precise mechanism was still unclear and needed to be studied in future research. In addition, there was no obvious deformation of morphology observed under SEM after six cycles (data not shown), demonstrating that the nanoflowers process very good mechanical stability.

In summary, a facile method was developed for synthesis of enzyme-inorganic hybrid nanoflowers. The synthetic method was simple and efficient, opening a new way for preparation of protein-inorganic hybrid nanoflowers. The resultant hybrid nanoflowers have hierarchical flower-like structure with high surface area and enhanced catalytic activity for small molecules. Furthermore, the resulting nanoflowers could be adopted as an IMER for the high-efficiency digestion of proteins. The successful applications suggest that the hybrid nanoflowers can be expected to be a promising IMER for proteomic analysis.

We gratefully acknowledge the financial support from the National Natural Science Foundation of China (21375018), the National Natural Science Foundation for Distinguished Young Scholar (21125524), the Program for Changjiang Scholars and Innovative Research Team in University (No. IRT1116).

Notes and references

- (a) C. Y. Chiu, Y. Li, L. Ruan, X. Ye, C. B. Murray and Y. Huang, *Nat. Chem.* 2011, **3**, 393-399; (b) S. Mann, *Nat. Mater.* 2009, **8**, 781-792; (c) L. B. Wang, Y. C. Wang, R. He, A. Zhuang, X. P. Wang, J. Zeng and J. G. Hou, *J. Am. Chem. Soc.* 2013, **135**, 1272-1275; (d) J. Y. Sun, J. C. Ge, W. M. Liu, M. H. Lan, H. Y. Zhang, P. F. Wang, Y. M. Wang and Z. W. Niu, *Nanoscale* 2014, **6**, 255-262.
- (a) A. C. Chen, X. S. Peng, K. Koczur and B. Miller Koczur, *Chem. Commun.* 2004, 1964-1965; (b) J. Tang and A. P. Alivisatos, *Nano Lett.* 2006, **6**, 2701-2706;
- (c) T. Tao, A. M. Glushenkov, H. W. Liu, Z. W. Liu, X. J. Dai, H. Chen, S. P. Ringer and Y. J. Chen, *J. Phys. Chem. C* 2011, **115**, 17297-17302; (d) H. Zhang, G. P. Cao, Z. Y. Wang, Y. S. Yang, Z. J. Shi and Z. N. Gu, *Nano Lett.* 2008, **8**, 2664-2668.
- J. Ge, J. D. Lei and R. N. Zare, *Nat. Nanotechnol.* 2012, **7**, 428-432.
- (a) A. Monzo, E. Sperling and A. Guttman, *TrAC, Trends Anal. Chem.* 2009, **28**, 854-864; (b) A. Papat, S. B. Hartono, F. Stahr, J. Liu, S. Z. Qiao and G. Q. Lu, *Nanoscale* 2011, **3**, 2801-2818.
- (a) S. Hudson, J. Cooney and E. Magner, *Angew. Chem. Int. Ed.* 2008, **47**, 8582-8594; (b) J. Ma, L. Zhang, Z. Liang, Y. Shan and Y. Zhang, *TrAC, Trends. Anal. Chem.* 2011, **30**, 691-702.
- R. Marangoni, R. Chiarini, G. Iannone and M. Salerno, *Proteomics* 2008, **8**, 2165-2167.
- (a) D. Li, W. Y. Teoh, J. J. Gooding, C. Selomulya and R. Amal, *Adv. Funct. Mater.* 2010, **20**, 1767-1777; (b) Y. Li, X. Q. Xu, C. H. Deng, P. Y. Yang and X. M. Zhang, *J. Proteome Res.* 2007, **6**, 3849-3855.
- (a) J. W. Cooper, J. Chen, Y. Li and C. S. Lee, *Anal. Chem.* 2003, **75**, 1067-1074; (b) J. Gao, Xu, J.; L. E. Locascio and C. S. Lee, *Anal. Chem.* 2001, **73**, 2648-2655.
- B. Bonnell, M. Mercier and K. C. Waldron, *Anal. Chim. Acta* 2000, **404**, 29-45.
- (a) J. Krekova, N. A. Lacher and F. Svec, *Anal. Chem.* 2009, **81**, 2004-2012; (b) J. F. Ma, Z. Liang, X. Q. Qiao, Q. L. Deng, D. Y. Tao, L. H. Zhang and Y. K. Zhang, *Anal. Chem.* 2008, **80**, 2949-2956; (c) J. F. Ma, C. Y. Hou, L. L. Sun, D. Y. Tao, Y. Y. Zhang, Y. C. Shan, Z. Liang, L. H. Zhang, L. Yang and Y. K. Zhang, *Anal. Chem.* 2010, **82**, 9622-9625.
- G. W. Schwert and Y. A. Takenaka, *Biochim. Biophys. Acta.* 1955, **16**, 570-575.
- (a) Y.-H. Shih, S.-H. Lo, N.-S. Yang, B. Singco, Y.-J. Cheng, C.-Y. Wu, I.-H. Chang, H.-Y. Huang and C.-H. Lin, *Chem Plus Chem.* 2012, **77**, 982-986; (b) Q. Min, R. A. Wu, L. Zhao, H. Qin, M. Ye, J. J. Zhu and H. Zou, *Chem. Commun.* 2010, **46**, 6144-6146; (c) M. T. Dulay, Q. J. Baca and R. N. Zare, *Anal. Chem.* 2005, **77**, 4604-4610; (d) M. Ethier, W. Hou, H. S. Duetwel and D. Figeys, *J. Proteome Res.* 2006, **5**, 2754-2759; (e) C. Temporini, E. Perani, E. Calleri, L. Dolcini, D. Lubda, G. Caccialanza and G. Massolini, *Anal. Chem.* 2007, **79**, 355-363.